J. Fluid Mech. (1967), *vol.* 29, *part* 4, *pp.* 625–645
Printed in Great Britain

The turbulence structure of equilibrium boundary layers

By P. BRADSHAW
Aerodynamics Division, National Physical Laboratory, Teddington

(Received 5 December 1966)

Measurements in three boundary layers, one with constant free-stream velocity and two with power-law variations of free-stream velocity giving 'moderate' and 'strong' adverse pressure gradients, are presented and discussed. Several unifying features of the turbulent motion, expected to appear in all boundary layers not too far from equilibrium, are identified. The intensity spectra at higher wavenumbers follow the Kolmogorov inertial-subrange law, although the Reynolds number is not particularly high even by laboratory standards: in addition the smaller-scale motion in the outer layer is determined entirely by the local shear stress and the boundary-layer thickness. The large eddy motion increases in strength relative to the general turbulence level as the general turbulence level increases, and the limited evidence available suggests that the large eddies are similar to those in the free mixing layer. In all cases the large eddies contribute a significant proportion of the shear stress in the outer layer.

1. Introduction

Equilibrium turbulent boundary layers are the nearest equivalent of the family of laminar boundary layers with similar profiles (Falkner–Skan flows). Exact similarity of profiles is possible only if the ratio of a typical eddy length scale, δ say, to a typical viscous length scale, ν/u_τ say, is constant, which is the case only in flow between converging planes. Even outside the viscous sublayer, the flow can be similar at different streamwise stations only if the surface shear-stress coefficient is nearly constant, although, for example, velocity-defect profiles in zero pressure gradient are found to be almost exactly similar, when plotted as $(U_1 - U)/u_\tau$ against the dimensionless distance from the surface y/δ, at Reynolds numbers easily attainable in the laboratory ($U_1\delta_2/\nu > 5000$, according to Coles (1962), where δ_2 is the momentum-deficit thickness). A necessary condition for similarity even of this restricted kind is that the contribution of the pressure gradient to the growth of the momentum deficit $\rho U_1^2\delta_2$ shall be a constant multiple of the contribution of the surface shear stress. Since

$$\frac{d}{dx}(\rho U_1^2\delta_2) = \tau_w + \delta_1\frac{dp}{dx},$$

where δ_1 is the displacement thickness, this implies $(\delta_1/\tau_w)dp/dx =$ constant, in compressible or incompressible flow. Townsend (1961) and Mellor & Gibson (1966) have shown that approximate similarity is obtained (in incompressible flow), if $U_1 \propto x^a$, as in laminar flow. In the present work we shall not distinguish between

boundary layers with $U_1 \propto x^a$, boundary layers with $(\delta_1/\tau_w)dp/dx \equiv \beta = \text{constant}$ and the ideal boundary layer (at infinite Reynolds number) with exactly similar defect profiles, because the difference between these three definitions of 'equilibrium' is within the experimental error: the nominal definition is $U_1 \propto x^a$.

In this paper, Clauser's (1954) work is extended by investigating the turbulence structure of equilibrium boundary layers in order to identify any universal relations between the various turbulence parameters. Since it is most unlikely that the internal processes of the random turbulent motion will be directly affected by departure from similarity of the mean velocity profiles, we expect the same universal relations to apply in all boundary layers not too far from equilibrium: the advantage of doing measurements in equilibrium boundary layers is that measurements need only be made at one station. Measurements have been made in the NPL boundary layer tunnel (Bradshaw & Hellens 1966) for three values of the exponent a, namely 0, $-0{\cdot}15$ and $-0{\cdot}255$, corresponding to $\beta \simeq 0$, $0{\cdot}9$ and $5{\cdot}4$ and representing zero pressure gradient, moderate adverse pressure gradient and strong adverse pressure gradient. It is unlikely that the continuously separating boundary layer investigated by Stratford (1959) differs greatly from the third boundary layer in its turbulence structure except near the surface. Boundary layers in strong *favourable* pressure gradients are dominated by the flow near the surface, where the universal 'mixing length' relations presumably apply, and are unlikely to manifest any new features.

The practical application of this work, together with that of Bradshaw (1965), is as an explanation and justification of the hypothesis used by Bradshaw, Ferriss & Atwell (1967), following Townsend (1961), in transforming the turbulent energy equation (see §7) into an equation for turbulent shear stress for use in predicting boundary-layer development in arbitrary pressure gradient. Their basic hypothesis was that the turbulent motion is uniquely related to the shear stress profile and independent, at least to a good first approximation, of the mean velocity profile past or present. Three extremely simple empirical functions were used to represent the turbulent intensity, its dissipation and diffusion entirely in terms of the shear stress: the definitions were respectively

$$a_1 = \tau/\overline{\rho q^2},$$
$$L = (\tau/\rho)^{\frac{3}{2}}/\epsilon,$$
$$G = (\overline{pv}/\rho + \tfrac{1}{2}\overline{q^2 v})/(\tau/\rho)(\tau_{\max}/\rho)^{\frac{1}{2}},$$

where $q^2 = u^2+v^2+w^2$ and u, v and w are the velocity fluctuations in the x (streamwise), y (normal) and z (transverse) directions.

The behaviour of the dimensionless parameter a_1, and of the dissipation length parameter L in the inner region of the boundary layer, has been discussed by Bradshaw (1965). In the present paper, the behaviour of L in the outer layer is inferred from the intensity spectra and the behaviour of G is discussed in relation to the large-eddy structure. The general nature of the turbulent energy balance is also discussed. These topics are embedded in a more general analysis of the experimental results. A somewhat fuller discussion, a description of the apparatus and larger-scale graphs are given in an earlier, unpublished version of this paper (Bradshaw 1966*a*).

2. General description of the boundary layers

In order to present large quantities of information in a small number of graphs, we have generally taken the liberty of omitting the experimental points. The scatter of the points is generally small, as can be seen from our other published papers, because an integrator is used to average the hot-wire readings over periods of 20 s or more: in any case, the scatter between points on a given run does not give any indication of absolute accuracy.

As was pointed out by Bradshaw & Ferriss (1965*b*), departures from two-dimensionality of the boundary layers in tunnels of reasonable width are confined to a slow convergence (or divergence) of the flow in the (x, z)-plane: true secondary flows only occur within a few boundary-layer thicknesses of the sidewalls (see

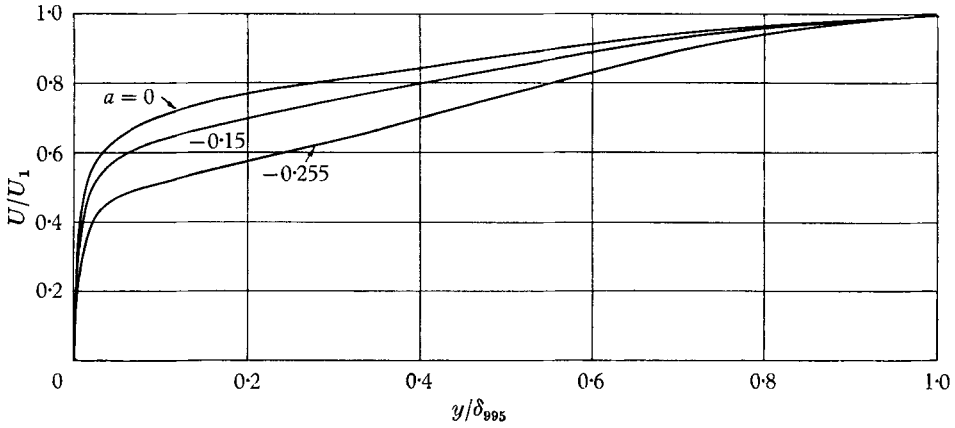

FIGURE 1. Mean velocity profiles, x = 83 in. (2·11 m).

figure 13 of Bradshaw & Hellens 1966). The virtual origin, $x = x_0$, of the convergence may be calculated by equating the imbalance in the two-dimensional momentum integral equation to $\delta_2/(x - x_0)$: the virtual origin was roughly 100 ft. (30 m) downstream of the working section for both the retarded boundary layers and x_0 may be assumed to be even greater for the boundary layer in zero pressure gradient. The effect of Reynolds normal stresses is comparatively small: even in the strongly retarded boundary layer they accounted for only 1 % of $d\delta_2/dx$, which must be regarded as within the error of measurement of the latter quantity.

The boundary-layer thicknesses at 83 in. (2.11 m) from the leading edge at a tunnel reference speed of 110 ft./s (34 m/s) and local free-stream speeds of 100–120 ft./s (30–37 m/s) were 1·25, 2·8 and 4·5 in. (0·032, 0·071, 0·114 m) respectively, so that the Reynolds number in the zero-pressure-gradient case was nearly the same as Klebanoff's (1955). All the measurements presented in the figures, except figure 3, were made at this station. The velocity profiles in the three boundary layers (figure 1) did not differ widely in shape ($H \equiv \delta_1/\delta_2$ = 1·34, 1·4, 1·54) and the difference in the behaviour of the flows is shown most clearly by the shear stress profiles (figure 2). It should be noted that the measurements are at different Reynolds numbers: the variation of surface shear stress coefficient $c_f = \tau_w/\frac{1}{2}\rho U_1^2$

with Reynolds number, as measured with Preston tubes using Head & Rechenberg's (1962) calibration, is shown in figure 3. Also in figure 3 are shown the variations with Reynolds number as given by

$$\frac{U_1}{u_\tau} = \sqrt{\frac{2}{c_f}} = \frac{1}{K}\log\frac{U_1\delta_1}{\nu} + c,$$

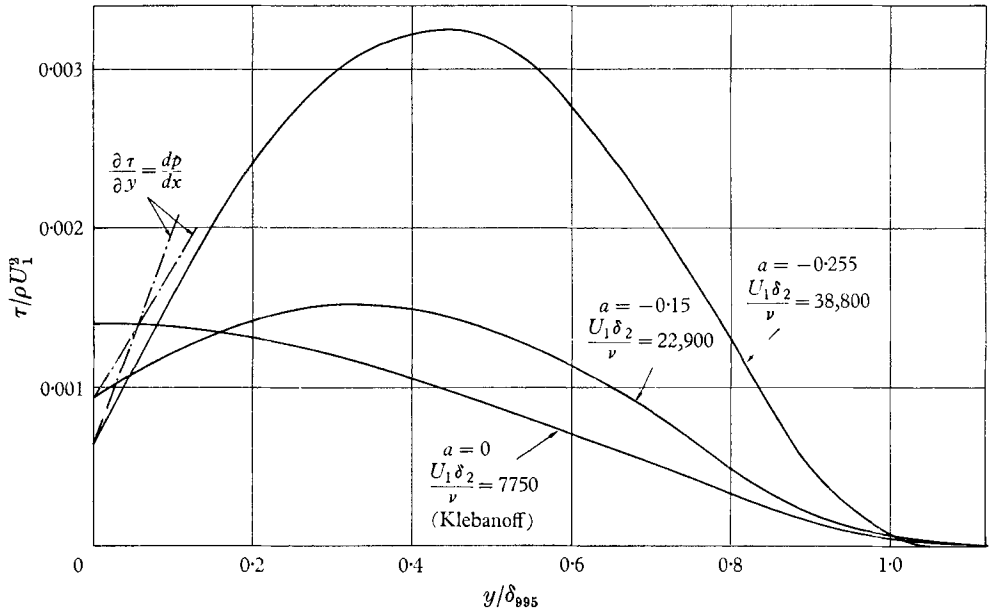

FIGURE 2. Shear stress profiles.

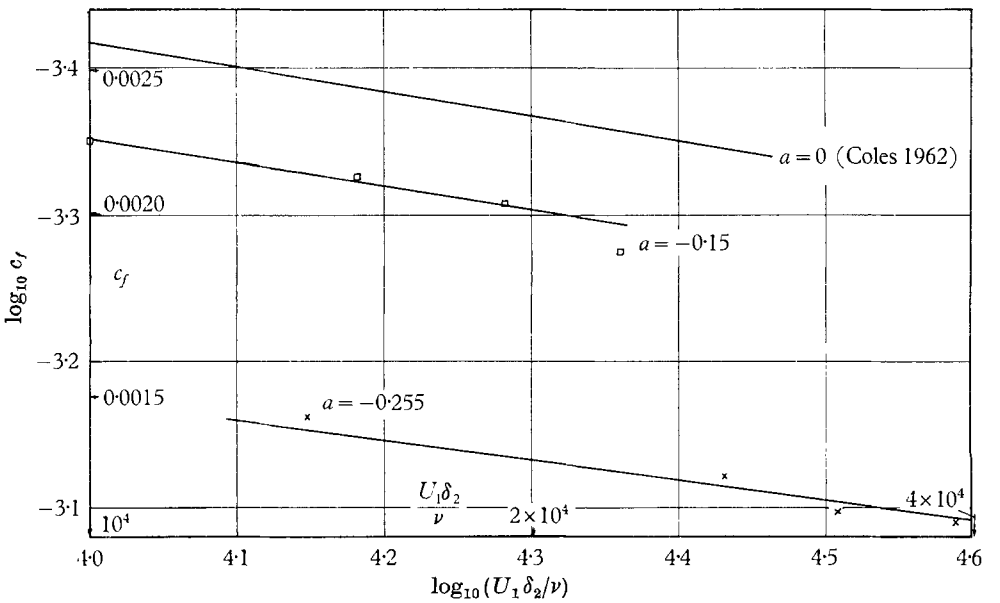

FIGURE 3. Surface shear stress coefficient $c_f = \tau_w/\frac{1}{2}\rho U_1^2$: lines are best fits of overlap law.

the surface shear-stress formula derived from the assumption of exact similarity of the defect profiles: K is taken as 0·41. At $U_1\delta_1/\nu = 2\times10^4$, the differences between the measured c_f and the Mellor–Gibson prediction for the same β are +4%, −1·2% and +6% for the three boundary layers. The accuracy of the predictions represents a convincing proof of the empirical constancy of the dimensionless eddy viscosity $\nu_T/U_1\delta_1$ over the whole range of equilibrium boundary layers.

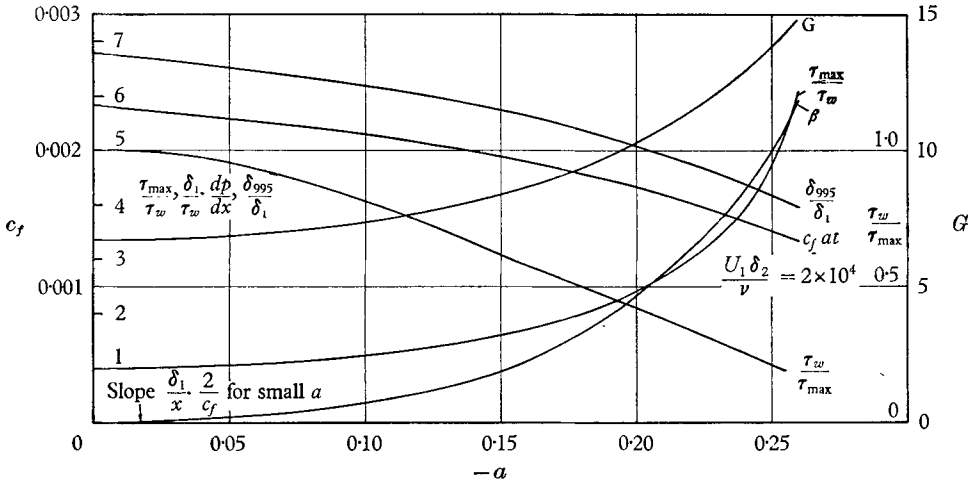

FIGURE 4. Boundary-layer parameters plotted against a.

In figure 4 some of the simpler boundary-layer parameters measured at $x = 83$ in. (2·11 m) are plotted against a, ignoring the effects of Reynolds number. Profile parameters and mean velocity profiles measured at different values of x are tabulated by Bradshaw (1966*a*).

The shear-stress profiles in figure 2 show that the *maximum* shear stress increases, with increasing pressure gradient, as the wall shear stress decreases. The shear-stress gradient near the wall is considerably smaller than the limiting value at the wall, $\partial\tau/dy = dp/dx$, which only applies if $|\rho U\,\partial U/\partial x| \ll |dp/dx|$ or $U \ll U_1$. The mixing length and eddy viscosity distributions are plotted in figures 5 and 6. It is seen that the eddy viscosity is far from constant in the outer part of the boundary layer and presumably tends to the molecular viscosity if τ represents total shear stress, although a tolerable approximation to the mean velocity profile is obtained by assuming a constant value. It was shown by Bradshaw & Ferriss (1965*b*) that a universal eddy viscosity $\nu_\tau/U_1\delta_1 = f(y/\delta)$ is compatible with a universal mixing length $l/\delta = f(y/\delta)$ if the velocity gradient is roughly constant over the outer portion of a given boundary layer. The universality emphatically does not apply to non-equilibrium boundary layers; the variations of dimensionless mixing length or eddy viscosity are not immense, but calculations of boundary-layer development in arbitrary pressure gradient using a universal mixing-length or eddy-viscosity function are not very satisfactory (although their predictions seldom fail as badly as those of the empirical momentum-integral methods in unusual pressure gradients).

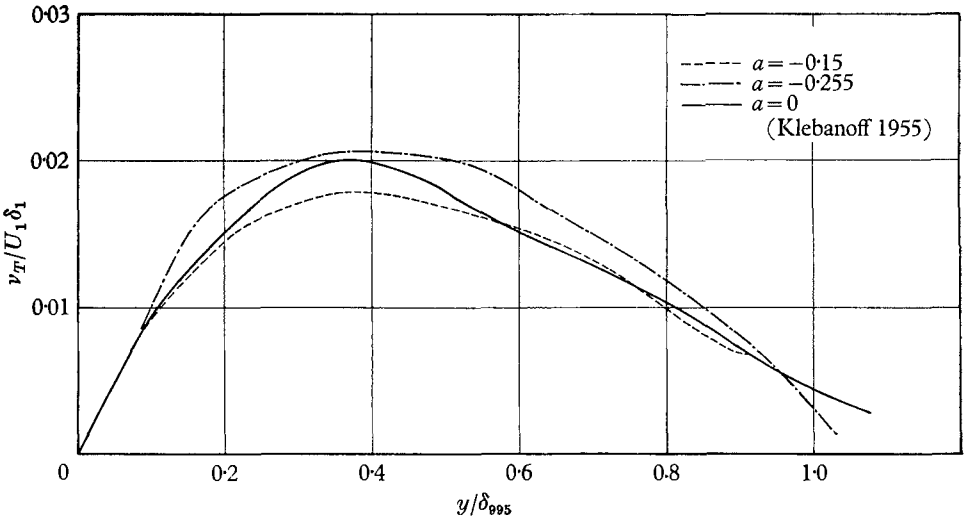

FIGURE 5. Eddy viscosity $\nu_T \equiv \tau/\rho\ (\partial U/\partial y)$.

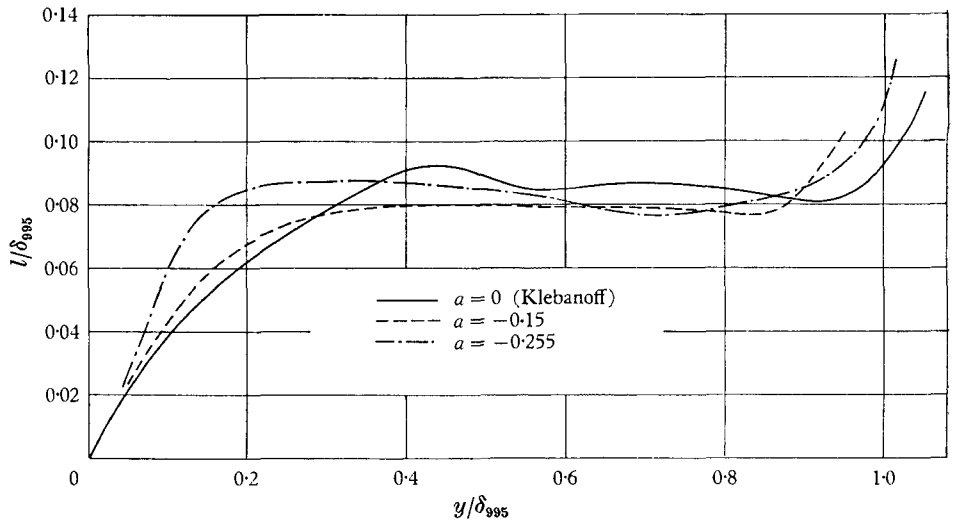

FIGURE 6. Mixing length $l \equiv (\tau/\rho)^{\frac{1}{2}}/(\partial U/\partial y)$.

3. The turbulent intensity and the function a_1

The inner layers in the boundary layers in zero pressure gradient and strong adverse pressure gradient were compared and discussed by Bradshaw (1965) who showed that the motion consists of an 'active' universal component scaling on $(\tau/\rho)^{\frac{1}{2}}$ and y, which produces the shear stress, and an 'inactive' component imposed by the eddies and pressure fluctuations in the outer part of the boundary layer, which does not produce shear stress and can be regarded as a quasi-steady oscillation of the inner layer flow. Measurements in the inner layer of the mildly retarded boundary layer do not add much to the qualitative picture: the strength of the inactive motion is intermediate between that in the other two boundary

layers, as can be seen from the intensity measurements in figure 7 and the values of $a_1 = \tau/\overline{\rho q^2}$ in figure 8 (here as elsewhere Klebanoff's measurements in zero pressure gradient have been used). Near the outer edge of the boundary layers, the irrotational motion becomes of comparable intensity to the turbulent fluctuations and a_1 again decreases. The irrotational motion, like the inactive motion which is closely related to it, increases in relative intensity as the boundary layer is more strongly retarded. In a quasi-infinite shear flow, in which the 'inactive' motion is minimal, the results of Rose (1966) indicate $a_1 \simeq 0{\cdot}18$.

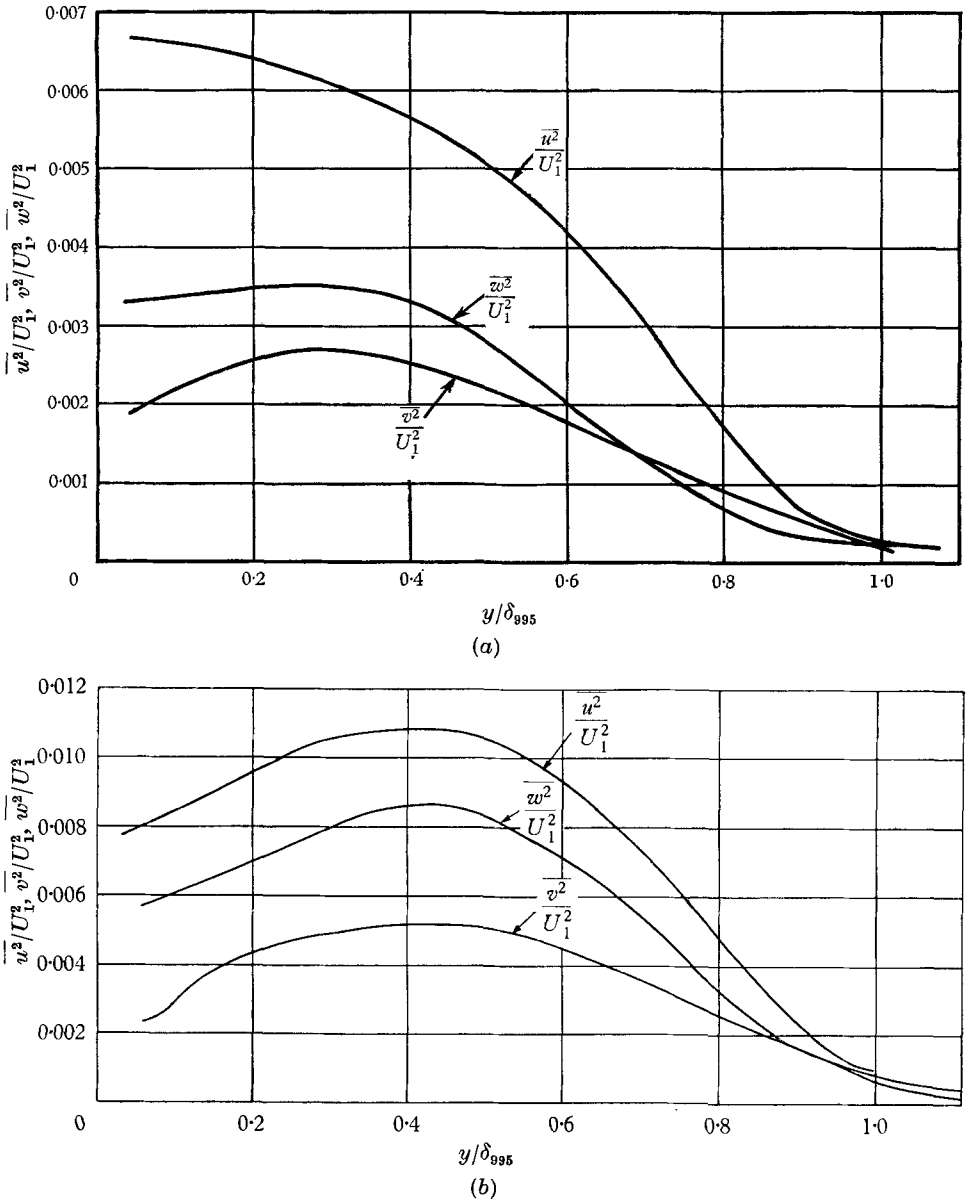

FIGURE 7. Turbulent intensity: (*a*) $a = -0{\cdot}15$, (*b*) $a = -0{\cdot}255$.

4. Intermittency and the outer-layer length scale

The intermittency in the retarded boundary layers, measured from oscilloscope film records, follows the usual error-function law as found by Klebanoff (1955) in zero pressure gradient, with a mean at $\bar{y}/\delta_{995} = 0{\cdot}86$, $0{\cdot}90$ and $0{\cdot}88$, and a standard deviation $\sigma/\delta_{995} = 0{\cdot}15$, $0{\cdot}14$ and $0{\cdot}18$ for $a = 0$, $-0{\cdot}15$ and $-0{\cdot}255$ respectively, where $U/U_1 = 0{\cdot}995$ at $y = \delta_{995}$. Since $\bar{y}$ is by definition the average distance of the laminar-turbulent interface from the surface it is the best possible choice for a

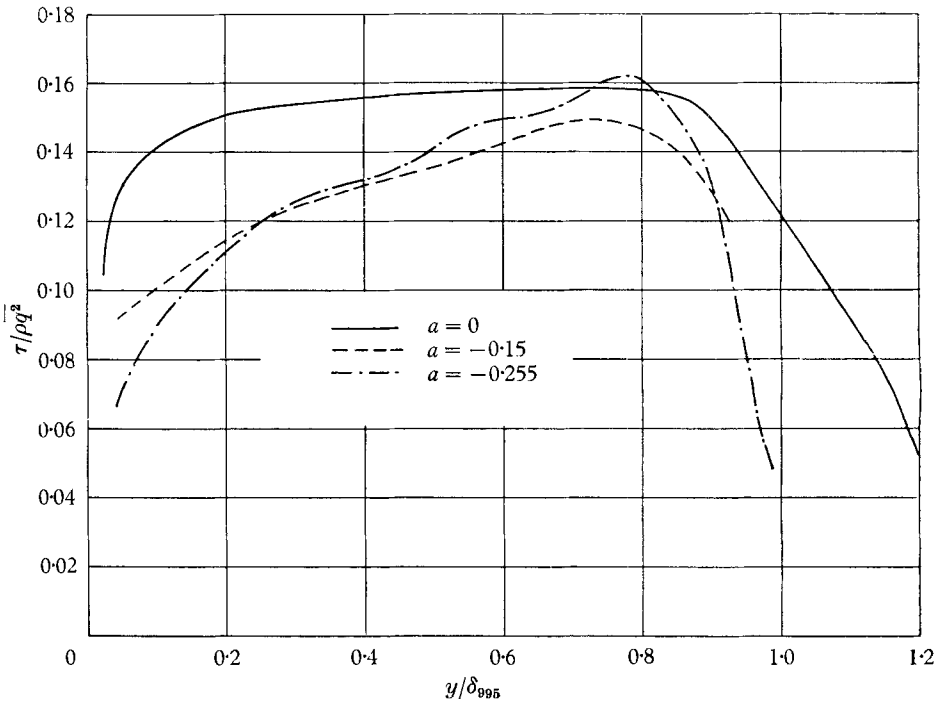

FIGURE 8. Ratio of shear stress to turbulent intensity.

length scale of the outer-layer motion. Gartshore (1966) has suggested that σ is a representative length scale of the large eddies, but if one thinks of the large eddies as 'mixing jets' (Grant 1958; see also §6 of the present paper) then σ is more closely related to a *velocity* scale of the large eddies, and the larger value of σ in the strongly retarded boundary layer, in which the large eddies are strongest, is compatible with this idea. The value of $\bar{y}/\delta_{995}$ is the same in all three boundary layers to within the likely accuracy of measurement, so that we may take δ_{995}, instead of $\bar{y}$, as a length scale for the outer layer motion, at least in equilibrium boundary layers. Fiedler & Head (1966) found that $\bar{y}/\delta_{995}$ increased monotonically with H in non-equilibrium retarded boundary layers at rather low Reynolds numbers, $U_1\delta_2/\nu < 5000$, reaching values close to unity near separation. It is difficult to believe that H is an adequate parameter for correlating details of the turbulent motion, but the results indicate that the large eddy structure of highly non-

equilibrium boundary layers may be different in scale from that of equilibrium boundary layers. However, the calculations of Bradshaw *et al.* (1967), assuming a universal length scale distribution, seem to agree well with experiment for a wide range of non-equilibrium boundary layers, so that the changes in length scale implied by Fiedler & Head's measurements may not be important in practice.

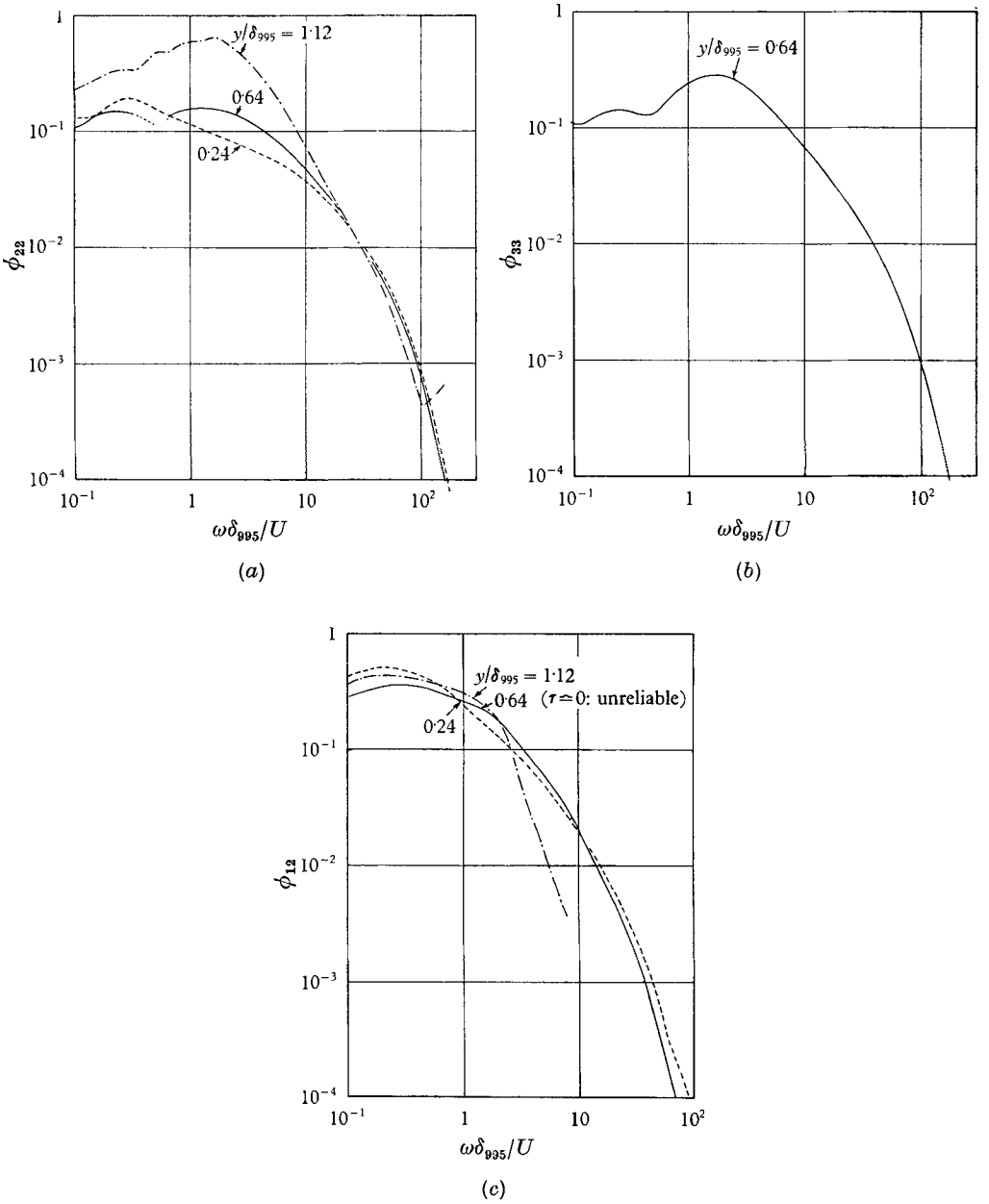

FIGURE 9. Spectral density made dimensionless with τ/ρ and δ_{995}: $a = 0$, (*a*) v-component, (*b*) w-component, (*c*) $\overline{uv}$ spectra.

5. The frequency spectra and the dissipation length parameter L

In the inner layer, as was mentioned in §3, the spectra of the 'active' motion scale on $(\tau/\rho)^{\frac{1}{2}}$ and y at all wave-numbers, as expected from the hypothesis of local equality of production and dissipation: it can be seen from the continuity equation that the additional motion imposed on the inner layer by the larger

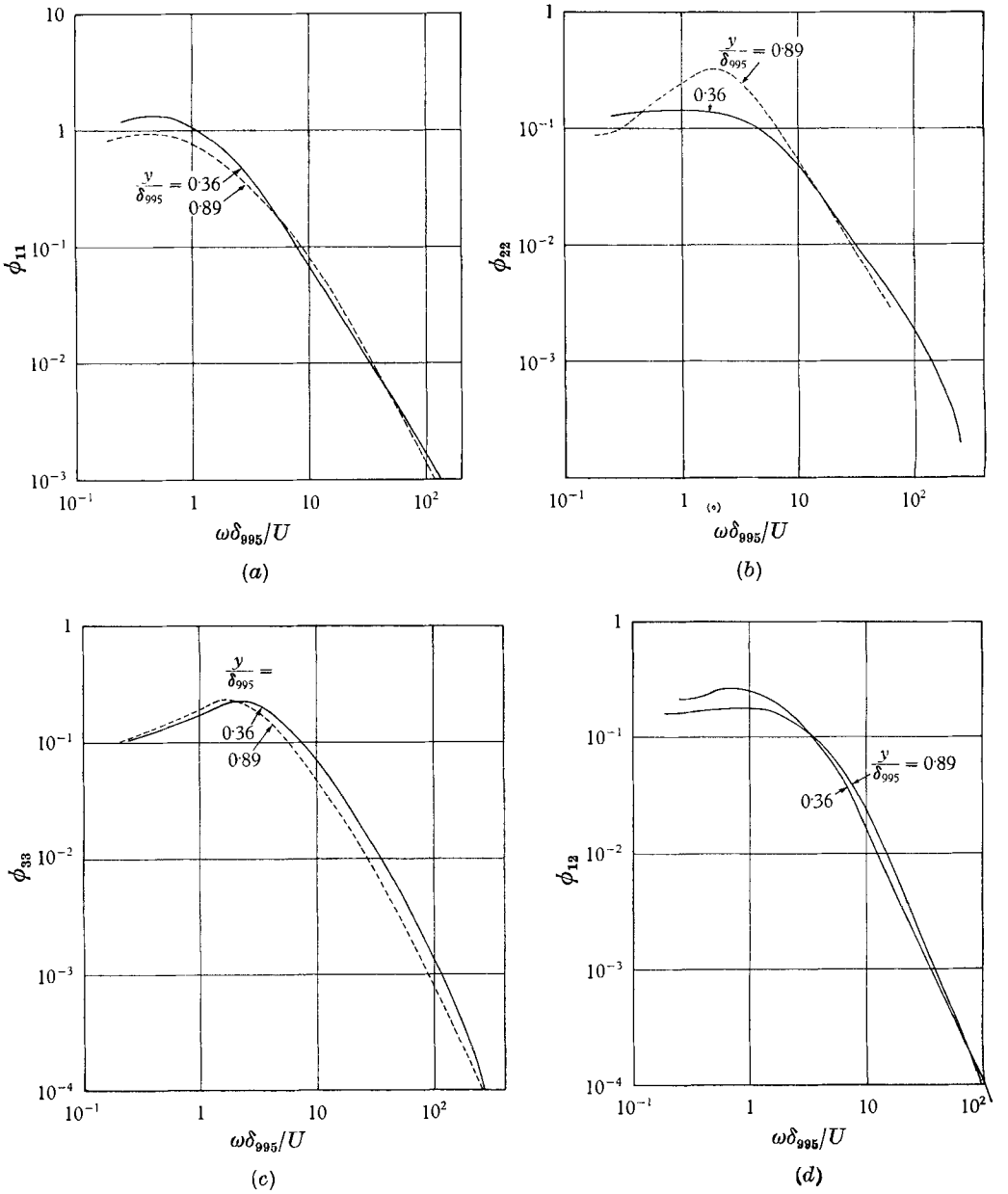

FIGURE 10. Spectral density made dimensionless with τ/ρ and δ_{995}: $a = -0{\cdot}15$. (*a*) u-component, (*b*) v-component, (*c*) w-component, (*d*) $\overline{uv}$ spectra.

eddies in the outer layer is mostly confined to the u and w components for distances from the surface small compared to a typical wavelength, and therefore does not contribute to the shear stress in the inner layer. In the outer layer, as will be seen below, a large part of the shear stress comes from the large eddies which extend over most of the width of the outer layer, and we cannot appeal to any ideas of local energy equilibrium to derive a velocity scale for the turbulent motion. However, because the large eddies produce a large part of the shear stress

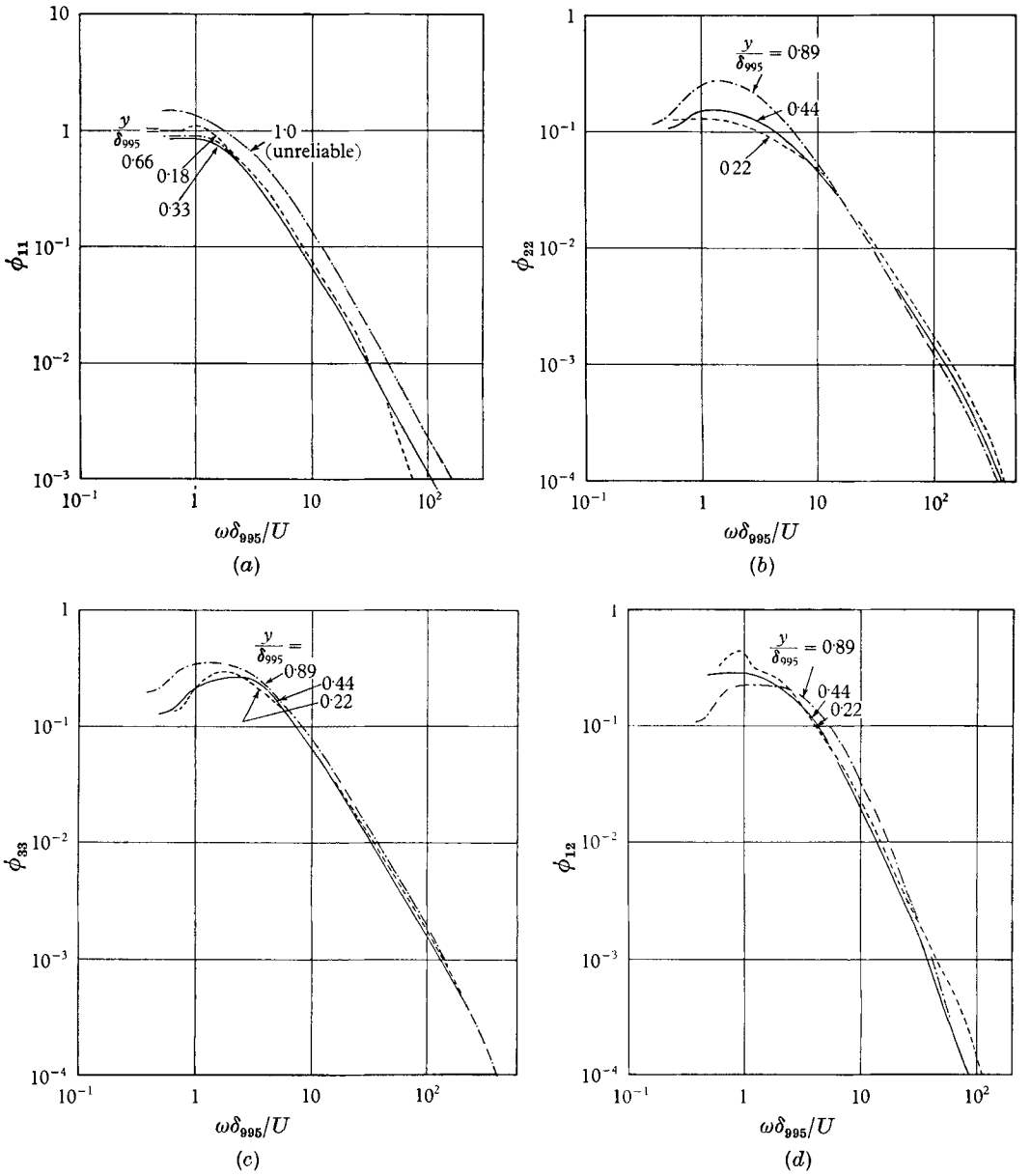

FIGURE 11. Spectral density made dimensionless with τ/ρ and δ_{995}: $a = -0{\cdot}255$. (*a*) u-component, (*b*) v-component, (*c*) w-component, (*d*) $\overline{uv}$ spectra.

and turbulence production they control the energy supply to the smaller eddies, so that we may expect $(\tau/\rho)^{\frac{1}{2}}$ to be an adequate velocity scale for the smaller eddies.

The frequency spectra in the outer layer are plotted in figures 9 to 11 against $\omega\delta_{995}/U$ ($\simeq k_1\delta_{995}$ where k_1 is the one-dimensional wave-number) the spectral density of u_iu_j, ϕ_{ij}, being made dimensionless by τ/ρ. The $\overline{v^2}$, $\overline{w^2}$ and $\overline{uv}$ spectrum measurements in zero pressure gradient, figure 9(*a*), (*b*) and (*c*), are new: *u*-component spectra have not been measured in this boundary layer in the present work but are given by Klebanoff (1955).

The higher-frequency parts of the spectra in the outer layers of each boundary layer collapse quite well together on these scales, generally rather better than on $\overline{u_i^2}$ and δ_{995}, but the collapse is not as good as the collapse on τ/ρ and y in the inner layer (Bradshaw 1965). Experimental scatter particularly affects the results near the outer edge where the shear stress is small, but apart from this it seems that the dimensionless spectral density tends to decrease towards the edge of the layer, indicating that in the 'outer layer', say the outer two-thirds of the boundary layer, the length scale gradually increases by 7–15 % (*or* alternatively the ratio of the velocity scale to $(\tau/\rho)^{\frac{1}{2}}$ decreases by 5–10 %). In addition, there is a slight decrease in spectral density as the boundary layer is more strongly retarded. However, it seems that for engineering purposes the higher-frequency motion, presumably including the dissipation, in a given boundary layer is a function only of the local shear stress and the overall thickness of the boundary layer, so that $L \propto \delta$ and $\epsilon \propto (\tau/\rho)^{\frac{3}{2}}/\delta$ within the turbulent fluid.

It is also noticeable that the spectral densities of the three components are nearly isotropically related at high frequencies and follow nearly the $-\frac{5}{3}$ power law predicted by Kolmogorov's theory (see, for instance, Batchelor (1953)). In the unpublished version of this paper the existence of local isotropy was dismissed, on the usual grounds that the shear correlation coefficient at a given wave number, $R_{12}(k) \equiv \phi_{12}/[\phi_{11}.\phi_{22}]^{\frac{1}{2}}$, was far from zero in the frequency range concerned, but further analysis of this and other data has led to the conclusion that the intensity spectra can follow the universal $-\frac{5}{3}$ law at a given wave-number k even though $R_{12}(k)$ is non-zero, provided that nearly all the production of turbulent energy occurs at wave-numbers below k and nearly all the dissipation at wave-numbers above k. Because the shear-stress spectral density is falling rapidly at the wave-numbers considered, this condition is compatible with non-zero $R_{12}(k)$. A more detailed discussion, and evidence that an inertial subrange occurs, in grid turbulence or shear flow, for microscale Reynolds numbers Re_λ greater than 90 (or $u_\tau y/\nu > 200$ in a boundary layer) is given by Bradshaw (1966*b*): the present results cover the range $100 < \mathrm{Re}_\lambda < 400$. Sandborn & Marshall (1965) have noted the presence of a $-\frac{5}{3}$ power-law region in the spectrum for $\mathrm{Re}_\lambda \geqslant 240$. It has yet to be explained why the energy transfer through the spectrum becomes isotropic at such low wave-numbers ($\omega\delta_{995}/U \sim 12$ say, a wavelength of fully half a boundary-layer thickness and as much as a sixth of the wavelength of the large eddies): the usual arguments about local isotropy postulate a wave-number ratio of more nearly 100 to 1 between the energy-containing eddies and the largest isotropic eddies. This is a quite different phenomenon from the *universality* of the

energy transfer, that is its proportionality to $(\tau/\rho)^{\frac{3}{2}}/\delta$. Whatever the explanation, the fact that the spectral density can be represented as $K'\epsilon^{\frac{2}{3}}k_1^{-\frac{5}{3}}$ (where $K' \simeq 0{\cdot}5$ for the u-component and $\frac{4}{3} \times 0{\cdot}5 = 0{\cdot}67$ for the v and w components) even at fairly modest laboratory Reynolds numbers provides us with a simple method of measuring turbulent dissipation and establishing the value of L in flows where it is not already known.

The near-universality of the energy transfer implies near-universality of the relation between turbulent energy production, shear-stress production and spectral transfer of energy in the larger eddies. This is *not* the same as universality of large-eddy scales (the low-frequency spectra certainly do not scale on τ) but can be crudely regarded as universality of large eddy correlation *shapes* so that the large-eddy motions in different equilibrium boundary layers differ only by scale factors of velocity and length. Evidently, equilibrium turbulent boundary layers comprise a sufficiently restricted range of flows for the turbulence structure to be nearly the same in each. For the turbulence structure to be similar in different parts of a given boundary layer it is necessary for an appreciable amount of turbulent diffusion to be effected by eddies with length scales of the same order as the boundary-layer thickness—this is the antithesis of the 'mixing length' concept of dependence on local conditions which is valid in the inner region of the boundary layer. This incidentally explains why the inner-layer spectra are so markedly different in *shape* from those in the outer layer as well as differing in scale.

6. The large-eddy structure and the diffusion function G

Townsend (1956), Grant (1958) and others have demonstrated that the large eddies in a turbulent shear flow form a coherent and identifiable group, and control the overall rate of spreading by contorting the boundary between the turbulent and non-turbulent fluid and by effecting bulk convection of turbulent energy from regions of maximum production. The qualitative concept is very useful, and immediately provides support for the ideas of the last paragraph. The large eddies in the outer part of a boundary layer do not seem to influence the inner layer, except in the 'inactive' sense of Bradshaw (1965): in the inner layer, the rapid variation of length scale with distance from the wall prevents the generation of any motion analogous to the large eddies in the outer layer. Townsend also hypothesized that, in a self-preserving flow, the large eddies should spend most of their lives in energy equilibrium, and derived a result which implies near-constancy of dimensionless eddy viscosity in all equilibrium boundary layers, as is experimentally observed: strictly, the energy-equilibrium analysis is valid only if the mean-flow momentum is constant during the life of a large eddy which is true only for free shear layers, but the error is probably small in boundary layers.

The actual intensity of the large eddies does not appear in the final results of the theory, but it is an implicit assumption of the theory that the large eddies do not themselves produce much of the shear stress, whereas in the above discussion we have implied that nearly all the shear stress occurs at frequencies below that at which the motion becomes universal. In the mixing layer it was found that

about a quarter of the area under the shear-stress frequency spectrum was accounted for by a peak, projecting above the general level of the spectrum, which was identified with the large eddy motion. The conclusion of Bradshaw, Ferriss & Johnson (1964) that the large eddies produced a quarter of the shear stress was a very conservative one, based on a rather naïve interpretation of one-dimensional spectra: whereas it is likely that a noticeable part of the energy at large-eddy wavelengths is not part of the group of eddies which produce the

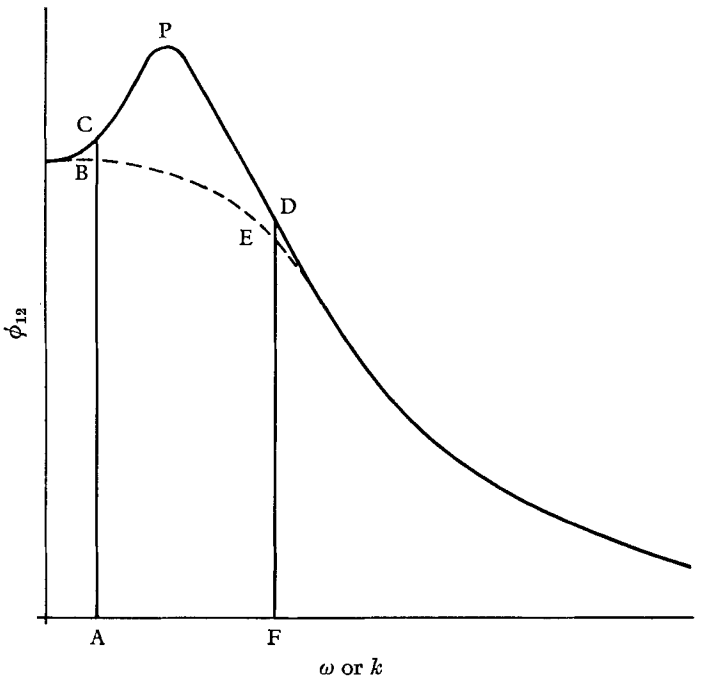

FIGURE 12. Contribution of large-eddy motion to shear stress: one-dimensional spectrum, linear scales.

peaks in the spectra, it is probable that the area ACPDF in figure 12 is a better approximation to the total energy of the coherent large eddies than the area BCPDE. This means that both in the mixing layer and at least the more strongly retarded boundary layers the large eddies produce a significant proportion of the total shear stress. Moreover, nearly all the shear stress occurs at frequencies less than three or four times the preferred frequency of the large eddies. Therefore, the assumption in the large-eddy equilibrium theory that the 'eddy viscosity' of the smaller-scale motion is equal to the eddy viscosity of the turbulence as a whole cannot be justified on Townsend's grounds. There is no reason to suppose that the eddy viscosities of the large-scale and small-scale eddies are equal. The reasonable quantitative agreement of the calculations with experiment cannot be invoked in support, because the large-eddy shape assumed by Townsend is not very like the mixing-jets found by Grant.

The large eddies increase in strength relative to the rest of the turbulence as the adverse pressure gradient and turbulence level increase, as can be seen from the

increasingly distinct peaks in the spectra in figures 9–11 respectively. Since the pressure gradient does not affect the flow directly, we must find a suitable measure of the 'turbulence level'. $\tau_{max}/\rho U_1^2$ will be used here, and has been found

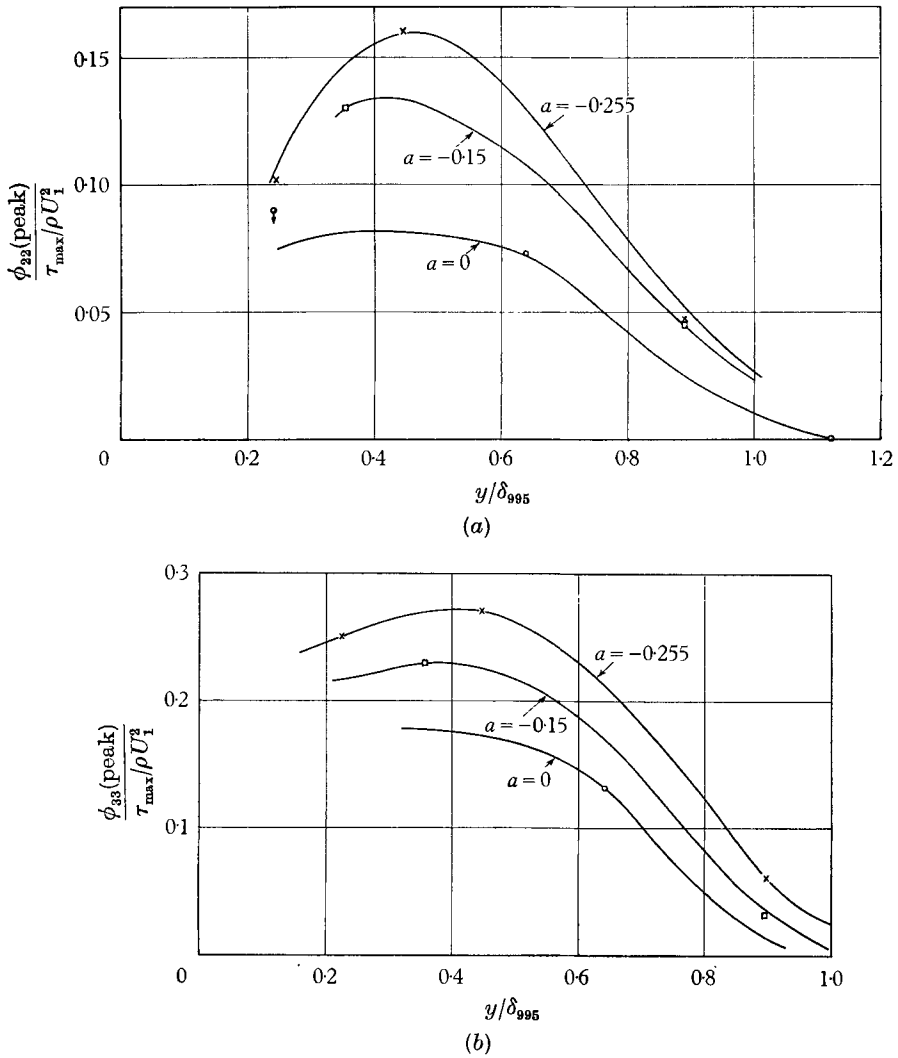

FIGURE 13. Ratio of peak spectral density to maximum shear stress. (*a*) *v*-component, (*b*) *w*-component.

to be adequate for correlating experimental data on the entrainment function G. By τ_{max} we really mean 'maximum shear stress in the outer part of the boundary layer', since the large eddy structure is not likely to be affected by a large shear stress in the small-scale turbulence near the wall such as occurs in accelerated boundary layers or boundary layers with suction.

The large eddy structure in the boundary layer in zero pressure gradient is noticeably less prominent than in the retarded boundary layers, although this is somewhat obscured in the present results because the lowest frequency measured,

16 c/s, is a much lower dimensionless frequency in the thinner boundary layer in zero pressure gradient whereas the spectra in the retarded boundary layers do not extend down to the region of constant spectral density at very low dimensionless

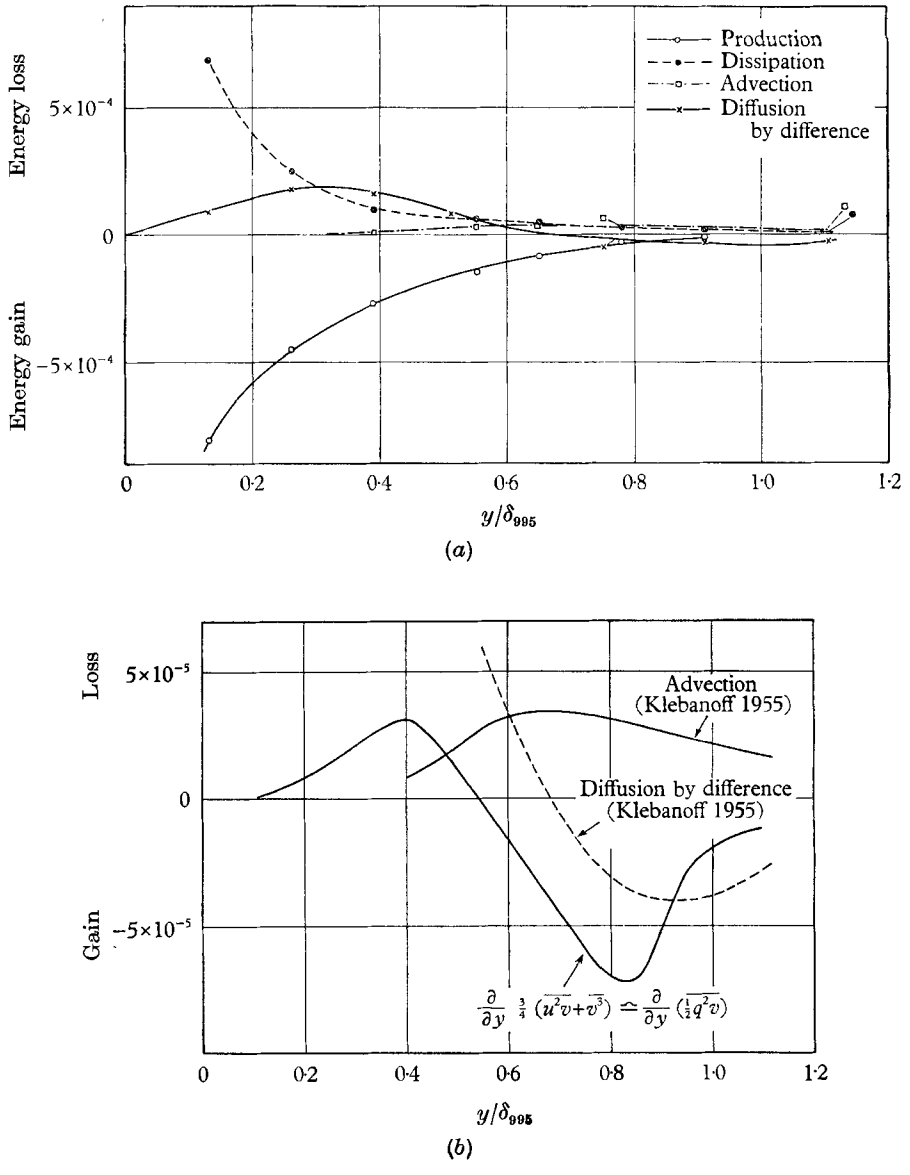

FIGURE 14(*a*), (*b*). For legend see facing page.

frequency. Figures 13(*a*) and (*b*) show the few available measurements of the peak spectral densities of the v and w component spectra in the three boundary layers, normalized by the *maximum* shear stress instead of the local shear stress. The three curves for a given component seem to be very roughly geometrically similar, but the overall level of spectral density increases much more quickly than

τ_{max}: many more spectrum measurements would be needed to define the trends more accurately.

A better overall measure of the strength of the large-eddy motion is the rate of diffusion of energy in the outer part of the boundary layer: at the edge of the

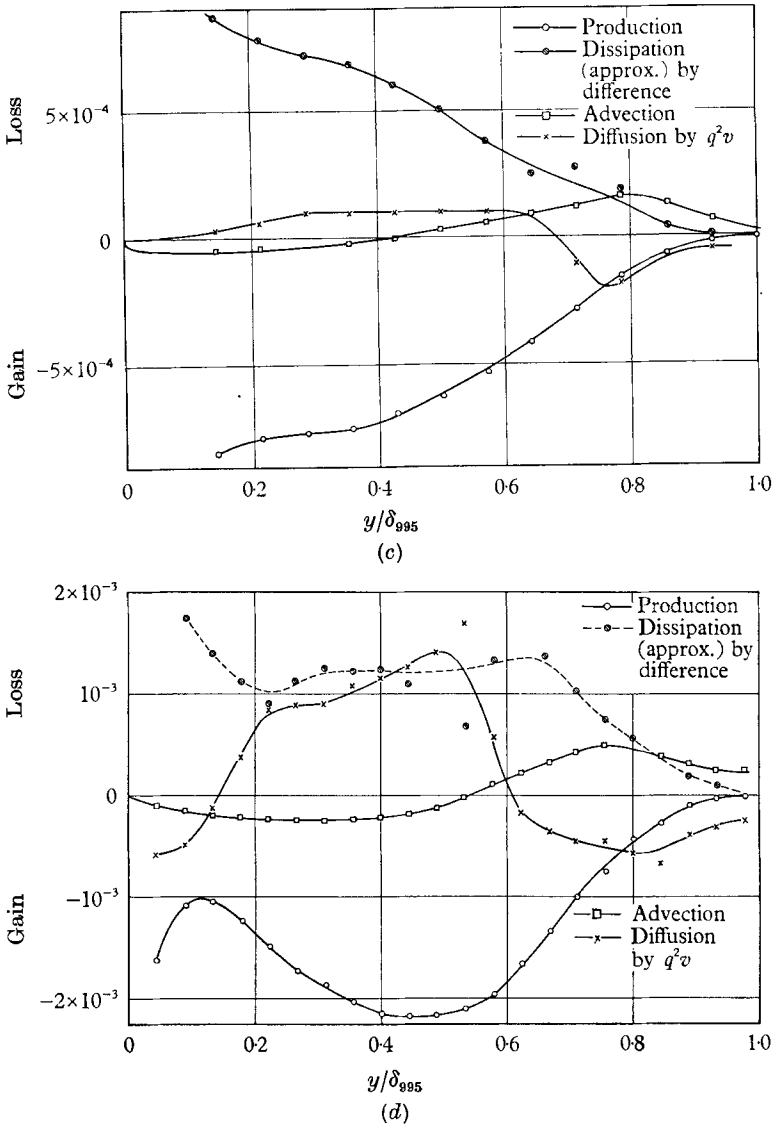

FIGURE 14. Turbulent energy balance. (*a*) $a = 0$, data of Klebanoff (1955); (*b*) $a = 0$, turbulent diffusion; (*c*) $a = -0{\cdot}15$; (*d*) $a = -0{\cdot}255$.

boundary layer, where the shear stress tends to zero and the energy balance therefore reduces to 'advection = diffusion', the rate of propagation of turbulent energy in the y direction is $\overline{pv}/\rho + \frac{1}{2}\overline{q^2v}$ so that a *velocity* of propagation V_p may be defined as

$$V_p = \frac{\overline{pv}/\rho + \frac{1}{2}\overline{q^2v}}{\frac{1}{2}\overline{q^2}}.$$

In a self-preserving boundary layer, V_p is equal to the mean rate of propagation of turbulent fluid into the free stream—the 'entrainment velocity'. Therefore

$$V_p = \frac{d}{dx} U_1(\delta - \delta_1)$$

which can be obtained from mean velocity measurements more easily than by direct measurement of turbulent diffusion. It is found empirically (Bradshaw *et al.* 1967) that V_p/U_1 is very nearly proportional to $(\tau_{\max}/\rho U_1^2)^{1\cdot0}$ both in equilibrium and non-equilibrium boundary layers and even in the mixing layer (at the high-velocity edge). If we take $(\tau_{\max}/\rho)^{\frac{1}{2}}$ as a suitable velocity scale for the smaller-scale turbulence in the central part of the boundary layer, justifying this by the fact that the spectra scale on local τ at the higher frequencies, it is implied that the ratio of the large-eddy velocity fluctuation to the smaller-scale velocity fluctuations in the central part of the boundary layer is proportional to $(\tau_{\max}/\rho U_1^2)^{0\cdot5}$ approximately.

The exact shape of the large eddies has been discussed for the boundary layer in zero pressure gradient and for the wake by Grant (1958) and for the free mixing layer by Bradshaw *et al.* (1964). In the wake and mixing layer, the large eddies take the form of 'mixing jets' or tongues of fluid erupting at more or less regular intervals into the irrotational flow. Grant felt that the evidence for quasi-periodic mixing jets in the boundary layer in zero pressure gradient was not entirely conclusive because the $R_{22}(r, 0, 0)$ correlation had a single negative loop instead of being periodic, but the v-component spectra in the outermost part of the boundary layer certainly show pronounced peaks, which imply a preferred periodicity: the peak is not noticeable in the spectrum at $y/\delta_{995} = 0\cdot53$, however, suggesting that the mixing jets only become observable in the extreme outer part of the boundary layer. All Grant's measurements were made at $y/\delta_{995} \leqslant 0\cdot5$. As the pressure gradient becomes more adverse the peak in the v-component spectra in the central part of the boundary layer becomes more obvious, which fits in with the suggestion above that the large eddies become proportionately stronger as the maximum shear stress increases. Judging by the spectra, the large eddy structure in the strongly retarded boundary layer ($\tau_{\max}/\rho U_1^2 \simeq 0\cdot003$) is a weaker version of that in the mixing layer ($\tau_{\max}/\rho U_1^2 \simeq 0\cdot01$) and it seems very likely that the large eddies take the form of mixing jets in boundary layers as well as in wakes and free mixing layers, because the strongly retarded boundary layer closely resembles a mixing layer in which mixing jets certainly exist, but a complete set of correlations in a retarded boundary layer would be necessary to clinch this.

7. The turbulent energy balance

The equation for the kinetic energy per unit mass of the turbulence, $\frac{1}{2}\overline{q^2}$, is

$$\left(U\frac{\partial}{\partial x} + V\frac{\partial}{\partial y}\right)\tfrac{1}{2}\overline{q^2} = \frac{\tau}{\rho}\frac{\partial U}{\partial y} - \frac{\partial}{\partial y}\left(\frac{\overline{pv}}{\rho} + \tfrac{1}{2}\overline{q^2 v}\right) - \nu\,\overline{u_i\frac{\partial^2 u_i}{\partial x_j^2}},$$

advection = production − diffusion − dissipation.

All numerical values presented here are in the dimensionless form obtained by multiplying the above equation by δ_{995}/U_1^3. Klebanoff (1955) has published an energy balance for the boundary layer in zero pressure gradient in which the dissipation was measured directly (that is, by measuring the microscales) and the diffusion obtained by difference. Direct dissipation measurements are very difficult and of doubtful reliability, whereas $\overline{q^2v} \equiv \overline{u^2v}+\overline{v^3}+\overline{w^2v}$ can be measured more straightforwardly, although it is a severe test of the linearizing circuits and the results have to be differentiated graphically to obtain the diffusion. The pressure diffusion cannot be measured at all, but it is certainly no larger than the velocity diffusion within the turbulent fluid and is probably much smaller, so that an estimate of the dissipation derived by neglecting the pressure diffusion and measuring all the other terms should not be seriously in error except near the edge of the boundary layer: in the irrotational field the dissipation is of course negligible and the advection is supplied entirely by pressure diffusion, so that the latter cannot be neglected when the intermittency is small.

The energy balances for the three boundary layers are plotted in figure 14(*a–d*). The differences are considerable: whereas the flow of energy in the outer part of the boundary layer in zero pressure gradient is so small as to be almost invisible on the graph (the same results are plotted, with a change of scale, as figure 10.2 of Townsend (1956)) the advection and diffusion in the outer part of the strongly retarded boundary layer are of the same order as the production and dissipation in the central part of the layer. The ratio of advection or diffusion to production in the outer part of the layer can be shown to be proportional to $\rho V_p^2/\tau$: since it was shown in §6 that V_p is roughly proportional to $\tau_{\max}/\rho U_1$ it follows that, at a given value of $\tau/\tau_{\max}$ (very roughly a given value of y/δ) the ratio of advection or diffusion to production is roughly proportional to $\tau_{\max}/\rho U_1^2$.

The quantity plotted as 'diffusion' in Klebanoff's results for zero pressure gradient is obtained by difference, using the measured dissipation. In the other two boundary layers, 'diffusion' is the gradient of $\frac{1}{2}\overline{q^2v}$ (neglecting $\overline{pv}$) and 'dissipation' is obtained by difference. Since Klebanoff's diffusion does not integrate to zero it is clearly inaccurate, and the large loss by diffusion from the inner half of the boundary layer is likely to be spurious: it certainly does not fit in with the trend of the other two boundary layers, nor with the 'diffusion', $\partial(\frac{1}{2}\overline{q^2v})/\partial y$, measured in the present experiments (figure 14(*b*)). This directly-measured diffusion does not integrate to zero either, because $\overline{q^2v}$ tended to a small positive value near the wall: since this implies a large loss by diffusion from the region very close to the wall it is probably an error.

The values of $\partial(\frac{1}{2}\overline{q^2v})/\partial y$ in the three boundary layers give a reasonably convincing representation of the *total* diffusion: for instance 'advection' $\simeq$ 'diffusion' near the outer edge as expected, so that the effect of $\partial(\overline{pv}/\rho)/\partial y$ is not very large even in this region. The value of $\overline{q^2v}$ diffusion in the inner half of the strongly retarded boundary layer seems to be considerably *higher* than the expected total diffusion: it is roughly equal to the dissipation and whereas these two terms are apparently nearly equal in the mixing layer (Bradshaw & Ferriss 1965*a*) one would not expect them to be equal in a boundary layer with only a third of the maximum shear stress. Moreover, the values of the dissipation length parameter L derived

from 'dissipation-by-difference' (figure 15) are considerably higher than the universal curve used successfully in calculations. It is possible that $\overline{pv}$ is of opposite sign to $\frac{1}{2}\overline{q^2v}$, as Lilley (1964) suggested it should be in the inner layer, but as $\overline{pv}$ is undoubtedly positive in the irrotational field outside the boundary layer its variation with y would be rather curious and it is difficult to visualize the physical mechanisms involved, partly because one cannot really consider $\overline{pv}$ separately from $\overline{q^2v}$. To within the accuracy of measurement of $\overline{q^2v}$, which is certainly rather poor, we may say that $\overline{pv}/\rho$ is negligible except of course in the irrotational field. The measurements of $\overline{q^2v}$ are given by Bradshaw (1965).

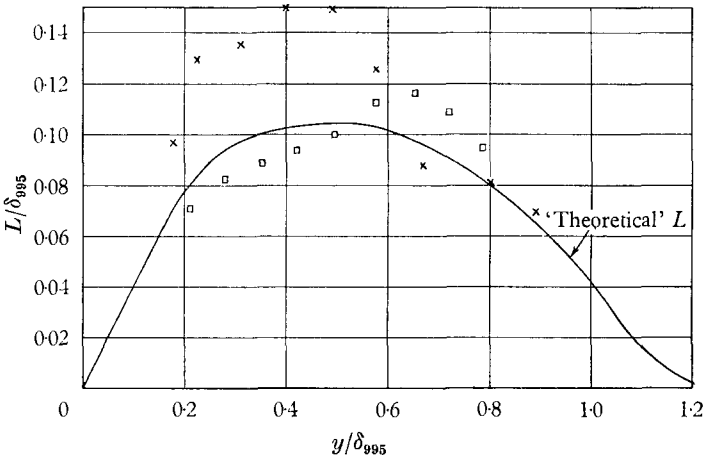

FIGURE 15. Dissipation length parameter $L = (\tau/\rho)^{\frac{3}{2}}/\epsilon$. □, $a = -0{\cdot}15$; ×, $a = -0{\cdot}255$.

It is interesting to note that production is roughly equal to dissipation in all parts of the three boundary layers except the outer edge (if one grants that the dissipation in the central part of the strongly retarded boundary layer is too small): the same result has been found in the calculations of Bradshaw *et al.* (1967). There is no real 'explanation' except that advection and diffusion are equal and opposite, to quite a good approximation, for $y/\delta > 0{\cdot}7$ and fairly small nearer the surface than this. It is implied that the dissipation length parameter L is nearly equal to the mixing length over most of the boundary layer so that the universality of L implies the universality of the mixing length—which is indeed observed. In non-equilibrium boundary layers the advection is *not* small for $y/\delta < 0{\cdot}7$, so that production is not nearly equal to dissipation and the mixing length is not nearly equal to the dissipation length parameter. The ideas of the present paper are epitomized by the claim that the dissipation length parameter, which connects two properties of the turbulence, is much more nearly universal than the mixing length, which ostensibly connects a property of the turbulence with a property of the mean flow.

Most of the experimental work was done by M. G. Terrell. D. H. Ferriss, G. K. Knight and P. C. Carpenter (vacation student, summer 1964) helped in the earlier stages of the work.

The work described in this paper forms part of the research programme carried out by the Aerodynamics Division of the National Physical Laboratory for the Ministry of Aviation.

REFERENCES

BATCHELOR, G. K. 1953 *The Theory of Homogeneous Turbulence*. Cambridge University Press.

BRADSHAW, P. 1965 *Nat. Phys. Lab. Aero Rept.* no. 1172 and *J. Fluid Mech.* (To be published.)

BRADSHAW, P. 1966*a* *Nat. Phys. Lab. Aero Rept.* no. 1184.

BRADSHAW, P. 1966*b* *Nat. Phys. Lab. Aero Rept.* no. 1220.

BRADSHAW, P. & FERRISS, D. H. 1965*a* *Aero. Res. Counc. Curr. Pap.* no. 899.

BRADSHAW, P. & FERRISS, D. H. 1965*b* *Nat. Phys. Lab. Aero Rept.* no. 1145.

BRADSHAW, P., FERRISS, D. H. & ATWELL, N. P. 1967 *J. Fluid Mech.* **28**, 593.

BRADSHAW, P., FERRISS, D. H. & JOHNSON, R. F. 1964 *J. Fluid Mech.* **19**, 591.

BRADSHAW, P. & HELLENS, G. E. 1966 *Aero. Res. Counc. R. & M.* no. 3437.

CLAUSER, F. H. 1954 *J. Aero. Sci.* **21**, 91.

COLES, D. 1962 *The RAND Corp., Rept.* no. R-403-PR.

FIEDLER, H. & HEAD, M. R. 1966 *J. Fluid Mech.* **25**, 719.

GARTSHORE, I. S. 1966 *J. Fluid Mech.* **24**, 89.

GRANT, H. L. 1958 *J. Fluid Mech.* **4**, 149.

HEAD, M. R. & RECHENBERG, I. 1962 *J. Fluid Mech.* **14**, 1.

KLEBANOFF, P. S. 1955 *Nat. Adv. Comm. Aero. Rept.* no. 1247.

LILLEY, G. M. 1964 *Arch. Mech. Stos.* **16**, 301.

MELLOR, G. L. & GIBSON, D. M. 1966 *J. Fluid Mech.* **24**, 225.

ROSE, W. G. 1966 *J. Fluid Mech.* **25**, 97.

SANDBORN, V. A. & MARSHALL, R. D. 1965 *Colorado State Univ. Research Memo*, no. 1.

STRATFORD, B. S. 1959 *J. Fluid Mech.* **5**, 17.

TOWNSEND, A. A. 1956 *The Structure of Turbulent Shear Flow*. Cambridge University Press.

TOWNSEND, A. A. 1961 *J. Fluid Mech.* **11**, 97.